

[DOI] 10.12016/j.issn.2096-1456.2023.01.008

· 临床研究 ·

下颌磨牙后管在山西人群中走形的影像学研究

弓前楠¹, 王珏², 范亚伟^{1,3}

1. 山西医科大学口腔医学院·口腔医院, 山西太原(030001); 2. 山西医科大学第一医院口腔修复科, 山西太原(030001); 3. 山西医科大学第一医院口腔颌面外科, 山西太原(030001)

【摘要】 目的 了解山西人群的下颌磨牙后管形态学特征, 测量相关数据, 为磨牙后区及下颌支部位手术安全性提供理论指导。方法 系统随机抽取山西医科大学第一医院口腔科400例患者锥形束CT影像资料, 筛选符合纳入标准影像, 使用锥形束CT及数字化软件测量相关数据, 进行磨牙后管分型, 建立磨牙后管三维模型, 观测并统计磨牙后管数量、分布及走形, 对相关数据进行测量。结果 本研究最终纳入样本368例, 84例样本中存在磨牙后管, 发生率为22.83%。其中男性47例, 女性37例; 左侧55例, 右侧52例, 性别、侧别间差异无统计学意义。以下颌角与磨牙后区后缘为界, 将磨牙后管起始位置分为A(下颌支区)、B(磨牙后区)两区, 磨牙后管按形态及走形可分为A1~A5、B1~B4共9型, 其中磨牙后管起自下颌支区沿下颌骨内侧弯曲向上行走的A3型最为多见, 其次是B3型, A4型最少见。磨牙后管平均长度为(10.95±2.76)mm, 起始位置平均直径为(1.22±0.50)mm, 磨牙后孔平均直径为(1.05±0.39)mm, 磨牙后孔距第三磨牙远中釉牙骨质界平均距离为(9.50±3.66)mm。结论 山西人群磨牙后管发生率较高, 行磨牙后区及下颌支部位手术时需避免术中术后并发症发生。

【关键词】 磨牙后管; 磨牙后孔; 锥形束CT; 下颌管分支; 分型; 发生率; 解剖变异

【中图分类号】 R78 **【文献标志码】** A **【文章编号】** 2096-1456(2023)01-0040-07

【引用著录格式】 弓前楠, 王珏, 范亚伟. 下颌磨牙后管在山西人群中走形的影像学研究[J]. 口腔疾病防治, 2023, 31(1): 40-46. doi:10.12016/j.issn.2096-1456.2023.01.008.

Imaging study of mandibular retromolar canal direction in Shanxi population GONG Qiannan¹, WANG Jue², FAN Yawei^{1,3}. 1. School and Hospital of Stomatology, Shanxi Medical University, Taiyuan 030001, China; 2. Department of Prosthodontics, the First Hospital, Shanxi Medical University, Taiyuan 030001, China; 3. Department of Oral and Maxillofacial Surgery, the First Hospital, Shanxi Medical University, Taiyuan 030001, China

Corresponding author: FAN Yawei, Email: yaweifan1970@163.com, Tel: 86-351-4639886

【Abstract】 Objective To study the morphological characteristics of the posterior canal of mandibular molars in the Shanxi population, provide theoretical guidance for the surgical safety of the retromolar region and mandibular ramus.

Methods A total of 400 patients in the Department of Stomatology of the First Hospital of Shanxi Medical University were randomly selected to screen the images that met the inclusion criteria. Cone beam computed tomography and digital software were used to measure the relevant data. Divide the classification of the retromolar canal, and establish a three-dimensional model of the retromolar canal. The number, distribution and course of the retromolar canals were observed and counted, and the relevant data were measured. **Results** A total of 368 samples were included in the study, and the retromolar canal was present in 84 samples, with an incidence of 22.83%. There were 47 men and 37 women; there were 55 on the left side and 52 on the right side, with no significant difference between the gender. In this study, the mandibular angle was bounded by the posterior margin of the retromolar region, and the initial position of the retromolar canal was divided into two regions: A (mandibular ramus area) and B (retromolar area). The retromolar canal can be divided into types A1 to A5 and B1 to B4 according to its shape and course, with type A3, which starts from the man-

【收稿日期】 2022-04-16; **【修回日期】** 2022-06-15

【基金项目】 国家自然科学基金项目(82003146)

【作者简介】 弓前楠, 学士, Email: 522385464@qq.com

【通信作者】 范亚伟, 主任医师, 硕士, Email: yaweifan1970@163.com, Tel: 86-351-4639886



微信公众号

dibular ramus area and bends upward along the medial side of the mandible, being the most common, followed by type B3, and type A4 being the least common. The mean length of the retromolar canal was (10.95 ± 2.76) mm, the mean diameter of the starting position was (1.22 ± 0.50) mm, the mean diameter of the retromolar foramen was (1.05 ± 0.39) mm, and the mean distance from the retromolar foramen to the distal enamel cementum boundary of the third molar was (9.50 ± 3.66) mm. **Conclusion** The incidence of retromolar canals is high in the population of Shanxi Province. It is necessary to note the presence of these canals in order to avoid intraoperative and postoperative complications when performing surgery on the retromolar region and mandibular ramus.

【Key words】 retromolar canal; retromolar foramen; cone beam CT; bifid mandibular canal; type; incidence; anatomic variation

J Prev Treat Stomatol Dis, 2023, 31(1): 40-46.

【Competing interests】 The authors declare no competing interests.

This study was supported by the grants from National Natural Science Foundation of China(No. 82003146).

下颌管是位于下颌骨骨松质间的骨性管道,该管起自下颌孔,向前下走形,止于颏孔,内含下牙槽神经及其伴行动静脉。以往观点认为下颌管是下颌骨内的一条单独管道结构,但近年来越来越多研究表明,下颌管存在分支结构,即下颌管分支(bifid mandibular canal, BMC)^[1]。根据 Naitoh 分类法^[2],下颌管分支可分为磨牙后管、牙管、前行管及颊舌侧管四型。其中磨牙后管(retromolar canal, RMC)是磨牙后区或下颌支部位的一种解剖变异,它起自下颌管,开口于磨牙后孔(retromolar foramen, RMF),其内包含有来源于下牙槽神经或颊长神经的有髓神经纤维及伴行小动静脉^[3]。磨牙后区及下颌支部位是临床下颌阻生第三磨牙拔除、自体骨移植、种植及正颌外科手术的重要区域^[4]。由于环境、饮食及种族差异等因素对下颌管生长发育的影响^[5],各国家和地区人群磨牙后管发生率不尽相同,比利时地区可达82.0%,伊朗约22.0%,埃及约7.5%^[6-8]。目前国内对磨牙后管的测量研究相对较少,且尚未对山西人群磨牙后管作出分型,本研究团队在下颌支部位取骨及磨牙后区牙槽外科手术中偶有出血严重的情况,也与磨牙后管密切相关,因此明确山西人群磨牙后管发生率及形态学特征具有重要临床意义。本研究通过锥形束CT(cone beam CT, CBCT)扫描患者颌面部数据,探讨山西人群磨牙后管发生率与性别、年龄及颌骨侧别间关系。同时观测磨牙后管走形,测量各位点间线性距离,划分磨牙后管分型,建立磨牙后管三维模型,为磨牙后区及下颌支部位手术安全性提供理论依据。

1 资料和方法

1.1 一般资料

系统随机抽取2020年1月至2021年1月山西医科大学第一医院口腔科400例籍贯及住址均为山西省的患者CBCT影像资料并筛选符合纳入标准影像。本研究最终纳入样本368例,纳入样本较均匀分布在山西省大部分地区,其中男性181例,女性187例;年龄18~75岁,平均40岁。按年龄划分,其中青年组(18~40岁)178例,中年组(41~65岁)167例,老年组(≥ 66 岁)23例。

1.2 样本选择

纳入标准:①年龄 ≥ 18 周岁;②颌面部基本对称,无畸形。排除标准:①CBCT图像不清晰,有严重金属伪影者;②未将关键截面包括在内的影像;③严重牙周炎、颌骨骨髓炎及影响下颌骨形态外伤、手术史;④颌骨囊肿及肿瘤等占位性病变。

1.3 样本拍摄

本研究受测者均使用同一台CBCT(New Tom-VGscanner, Verona公司,意大利)进行拍摄。患者保持站立位,将头部固定,取正中颌,使患者眶耳平面与地平面平行,面中线与地平面垂直。扫描参数设置为:电压110 kV,电流0.71~1.62 mA,分辨率0.30 mm,扫描区间15 cm \times 15 cm。采用自带图像分析软件NNT viewer(QRs.r.l, Verona公司,意大利)、SIMPLANT PRO 17.01软件对CBCT影像进行三维方向测量分析;采用SIMPLANT PRO 17.01软件描记下颌管及磨牙后管走形,建立磨牙后管三维模型。

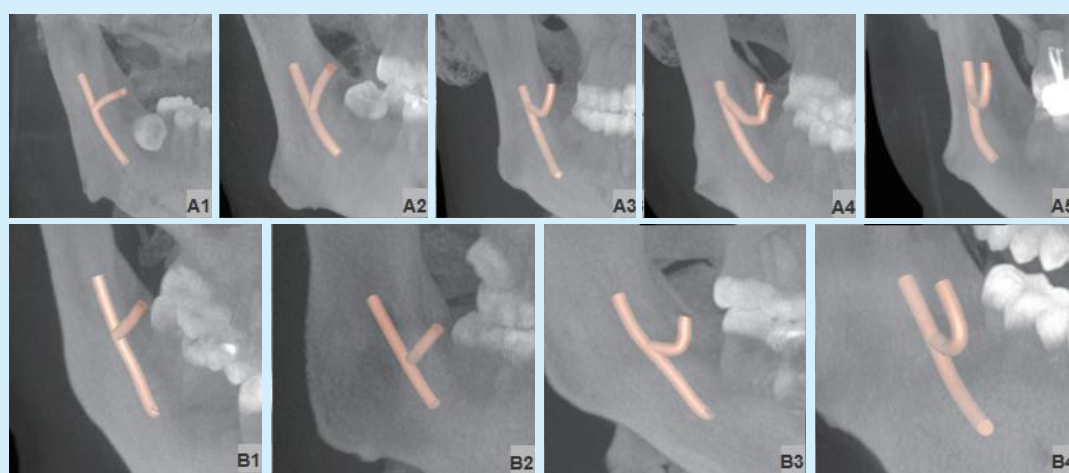
1.4 测量内容

1.4.1 磨牙后管发生率 下颌管分支出现的标志是

有“骨岛”的存在,骨岛即两条神经管相接位置形成的一个三角形,三角形的顶点代表两条神经的分离点^[1]。通过调整CBCT影像灰度、锐度以及观测平面角度,分别于冠状面、矢状面、水平面上仔细辨认磨牙后管的存在,统计磨牙后管发生率。

1.4.2 磨牙后管分型 本研究以下颌角与磨牙后区后缘为界,将磨牙后管起始位置分为A(下颌支区)、B(磨牙后区)两区,使用SIMPLANT PRO 17.01软件在三维空间上将磨牙后管分为A1~A5、B1~B4共9型(图1)。A1型:磨牙后管起自A区,沿下

颌骨内侧直线向上;A2型:磨牙后管起自A区,沿下颌骨外侧直线向上;A3型:磨牙后管起自A区,沿下颌骨内侧弯曲向上;A4型:磨牙后管起自A区,沿下颌骨内侧弯曲向上,途中发出前后两个分支;A5型:磨牙后管起自A区,沿下颌骨外侧弯曲向上;B1型:磨牙后管起自B区,沿下颌骨内侧直线向上;B2型:磨牙后管起自B区,沿下颌骨外侧直线向上;B3型:磨牙后管起自B区,沿下颌骨内侧弯曲向上;B4型:磨牙后管起自B区,沿下颌骨外侧弯曲向上。



Bounding by the mandibular angle and posterior margin of the retromolar region, the retromolar canal is divided into two types: A and B. A1: the retromolar canal arises from mandibular and straights upward along the medial mandible; A2: the retromolar canal arises from mandibular and straights upward along the lateral mandible; A3: the retromolar canal arises from mandibular and curves upward along the medial mandible; A4: the retromolar canal arises from mandibular and curves upward along the medial mandible, giving rise to two branches before and after on the way; A5: the retromolar canal arises from mandibular and curves upward along the lateral mandible; B1: the retromolar canal arises from retromolar and straights upward along the medial mandible; B2: the retromolar canal arises from retromolar and straights upward along the lateral mandible; B3: the retromolar canal arises from retromolar and curves upward along the medial mandible; B4: the retromolar canal arises from retromolar and curves upward along the lateral mandible

Figure 1 Three-dimensional classification of retromolar canal

图1 磨牙后管三维分型

1.4.3 磨牙后管数据测量 ①磨牙后管水平长度(L1):磨牙后管起始位置中心点距磨牙后孔中心点距离;②磨牙后管垂直高度(H):磨牙后孔中心点距下颌管上缘的垂直距离;③磨牙后孔中心点距下颌第三磨牙远中釉牙骨质界(CEJ)距离(L2);④磨牙后管起始位置中心点距颊侧骨壁的水平距离(L3);⑤磨牙后管起始位置中心点距舌侧骨壁的水平距离(L4);⑥磨牙后孔中心点距颊侧骨壁的垂直距离(L5);⑦磨牙后孔中心点距舌侧骨壁的垂直距离(L6);⑧磨牙后管起始位置直径(D1);⑨磨牙后孔直径(D2),见图2。数据测量由同一测量者在同一台电脑上进行,重复3次,取平均值。

测量间隔2个月,测量数据需随机排序,防止测量者记忆误差。

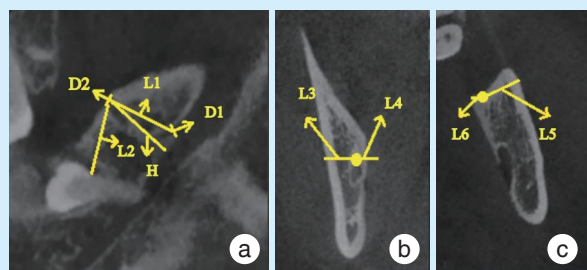
1.5 统计学方法

运用SPSS 28.0软件对测量数据进行统计学分析,各点位间距离用均值±标准差表示,性别、侧别及年龄组的比较采用卡方检验,检验水准 $\alpha = 0.05$ 。

2 结果

2.1 磨牙后管发生率及分型

本研究368例(736侧)样本中,84例(107侧)样本存在磨牙后管,人群中发生率为22.83%。其中男性47例,女性37例,磨牙后管在性别间的分



a: the sagittal linear measurement data of the retromolar canal; L1: the horizontal length of the retromolar canal; H: the vertical height of the retromolar canal; L2: the distance from the center point of the retromolar foramen to the distal cemento-enamel junction of the mandibular third molar; D1: the diameter of the starting position of the retromolar canal; D2: the diameter of the retromolar foramen; b: the coronal linear measurement data of the retromolar canal; L3: the horizontal distance from the center point of the retromolar canal to the buccal bone wall; L4: the horizontal distance from the center point of the retromolar canal to the lingual bone wall; c: the horizontal linear measurement data of the retromolar canal; L5: the vertical distance from the center point of the retromolar foramen to the buccal bone wall; L6: the vertical distance from the center point of the retromolar foramen to the lingual bone wall

Figure 2 Measurement of retromolar canal data

图2 磨牙后管在三维方向上的测量数据

布差异无统计学意义($\chi^2 = 1.995, P = 0.158$);在各年龄组中,青年组发现37例,中年组43例,老年组4例,各组磨牙后管发生率分别为20.79%、25.75%、17.39%,磨牙后管在各年龄组间的分布差异无统计学意义($\chi^2 = 1.616, P = 0.446$);在侧别分布中,左侧55侧,右侧52侧,磨牙后管在侧别间的分布差异无统计学意义($\chi^2 = 0.098, P = 0.754$),见表1。

磨牙后管A区分型中,A1~A5型比率分别为6.54%、2.80%、52.34%、0.93%、2.80%,B1~B4型比率分别为3.74%、1.87%、26.17%、2.80%,磨牙后管在A区和B区占比分别为:65.42%、34.58%,差异有统计学意义($\chi^2 = 10.975, P = 0.001$),见表2。

2.2 磨牙后管线性测量数据

本研究显示磨牙后管长度平均为(10.95 ± 2.76)mm,磨牙后孔中心点距第三磨牙远中釉牙骨质界距离平均为(9.50 ± 3.66)mm,磨牙后管起始位置中心点距颊侧骨壁的水平距离平均为(7.30 ± 1.99)mm;磨牙后管起始位置中心点距舌侧骨壁的水平距离平均为(3.51 ± 1.04)mm,磨牙后管起始位置中心点距颊舌侧骨壁的水平距离差异有统计学意义($P < 0.001$);磨牙后孔中心点距颊侧骨壁的垂直距离平均为(8.22 ± 2.18)mm;磨牙后孔中心

表1 磨牙后管性别、年龄及侧别分布

Table 1 Gender, age and lateral distribution of retromolar canal

	Presence	Absence	Total	Incidence(%)	χ^2	<i>P</i>
Gender						
Male	47	134	181	25.97	1.995	0.158
Female	37	150	187	19.79		
Age/year						
18-40	37	141	178	20.79	1.616	0.446
41-65	43	124	167	25.75		
≥66	4	19	23	17.39		
Lateral						
Left	55	313	368	14.95	0.098	0.754
Right	52	316	368	14.13		

表2 磨牙后管各分型占比

Table 2 Percentage of each type of retromolar canal

Type	Number of sides	Left/right	Ratio(%)	χ^2	<i>P</i>
A1	7	4/3	6.54	10.975	0.001
A2	3	2/1	2.80		
A3	56	31/25	52.34		
A4	1	0/1	0.93		
A5	3	1/2	2.80		
B1	4	3/1	3.74		
B2	2	1/1	1.87		
B3	28	11/17	26.17		
B4	3	2/1	2.80		
Total	107	55/52	100		

Bounding by the mandibular angle and posterior margin of the retromolar region, the retromolar canal is divided into two types: A and B (as Figure 1). Type A1: the retromolar canal arises from region A and straightens upward along the medial mandible; type A2: the retromolar canal arises from region A and straightens upward along the lateral mandible; type A3: the retromolar canal arises from region A and curves upward along the medial mandible; type A4: the retromolar canal arises from region A and curves upward along the medial mandible, giving rise to two branches before and after on the way; type A5: the retromolar canal arises from region A and curves upward along the lateral mandible; type B1: the retromolar canal arises from region B and straightens upward along the medial mandible; type B2: the retromolar canal arises from region B and straightens upward along the lateral mandible; type B3: the retromolar canal arises from region B and curves upward along the medial mandible; type B4: the retromolar canal arises from region B and curves upward along the lateral mandible

点距舌侧骨壁的垂直距离平均为(3.87 ± 1.77)mm,磨牙后孔中心点距颊舌侧骨壁的垂直距离差异有统计学意义($P < 0.001$)。起始位置直径平均为(1.22 ± 0.50)mm,磨牙后孔直径平均为(1.05 ± 0.39)mm,见表3。

表3 磨牙后管线性测量数据

Table 3 Linear measurement data of molar

Item	posterior canal		mm
	Minimum value	Maximum value	
L1	6.61	17.88	10.95 ± 2.76
L2	5.02	19.10	9.50 ± 3.66
L3	3.90	10.13	7.30 ± 1.99 ^a
L4	2.68	6.30	3.51 ± 1.04 ^a
L5	4.70	11.98	8.22 ± 2.18 ^b
L6	1.55	7.30	3.87 ± 1.77 ^b
D1	0.43	3.07	1.22 ± 0.50
D2	0.47	2.02	1.05 ± 0.39

a: L3 vs. L4, $P < 0.001$; b: L5 vs. L6, $P < 0.001$. L1: the horizontal length of the retromolar canal; L2: the distance from the center point of the retromolar foramen to the distal cemento-enamel junction of the mandibular third molar; L3: the horizontal distance from the center point of the retromolar canal to the buccal bone wall; L4: the horizontal distance from the center point of the retromolar canal to the lingual bone wall; L5: the vertical distance from the center point of the retromolar foramen to the buccal bone wall; L6: the vertical distance from the center point of the retromolar foramen to the lingual bone wall; D1: the diameter of the starting position of the retromolar canal, D2: the diameter of the retromolar foramen

3 讨论

3.1 磨牙后管形成原因

磨牙后管形成原因目前尚未阐明,多数人认可的是Chávez-Lomeli等^[9]提出的神经小管不全融合理论。该理论指出在胚胎时期,下颌骨内会形成3条神经管道,分别支配下前牙、前磨牙及磨牙,这种管道结构被称为神经小管。随着胎儿发育及下颌骨膜内成骨,神经小管逐渐融合,最终形成一条单独的管道结构,即下颌管。如果神经小管融合不全,则会出现磨牙后管等变异解剖结构。

3.2 研究方法、磨牙后管分型及发生率

国内外学者通过下颌骨解剖标本、组织病理学、影像学方法等多种方式对磨牙后管进行研究。通过下颌骨解剖标本,可以直观地判断磨牙后管的起始位置、走形、管径大小,磨牙后孔位置及直径;同时也可通过研究不同发育阶段下颌骨内管道结构走形,探究磨牙后管的形成原因^[9-11]。有学者通过对下颌骨标本内下颌管及其分支内容物进行组织病理学研究发现,磨牙后管内存在有髓神经纤维及伴行动静脉,损伤磨牙后管可引起磨牙后区感觉异常及术区出血等并发症发生^[3, 12]。但受样本量限制和解剖标本由于长时间

干燥、风化造成的损害,这两种方法对磨牙后管发生率的评估以及对相关数据的测量存在一定的误差^[13]。既往有学者通过曲面体层片研究磨牙后管,但由于曲面体层片只显示二维影像,成像存在扭曲变形、影像重叠等缺点,磨牙后管易与骨小梁、下颌舌骨嵴等解剖结构影像相混淆^[14];同时磨牙后管的管径大小及走形也会对观测造成一定程度影响,因而通过曲面体层片观测难以发现磨牙后管的存在,发生率仅为0.79%~0.90%,曾被学者认为是一种少见的解剖变异^[15]。随着影像学技术的发展,目前CBCT已广泛应用于口腔颌面部疾病诊治过程,它具有空间分辨率高、扫描速度快、放射剂量低等优点,可从任意角度对影像进行三维重建,其扫描精度为0.1~0.3 mm,能够清晰显示颌骨内各解剖结构^[16]。CBCT相较曲面体层片可以更加清晰地显示磨牙后管的存在,且可以观察其在三维方向上的走形,对磨牙后管发生率的评估也更加准确。通过CBCT观测到磨牙后管发生率为7.5%~82.0%,可见其并非罕见。目前多数学者认为,曲面体层片无法准确诊断磨牙后管的存在,在曲面体层片上发现可疑磨牙后管影像时,需通过CBCT行进一步诊断。

以往学者多采用Patil分类法^[17]在矢状面上将磨牙后管分为3种主要类型:①A型为低位型,即磨牙后管自下颌管发出,于下颌第三磨牙远端向上,止于磨牙后区,开口于磨牙后孔,该型可分为A1、A2两类亚型,A1型磨牙后管以直线方式向上延伸至磨牙后区,A2型磨牙后管以弯曲的方式向前延伸至磨牙后区;②B型为根端型,该型磨牙后管起自下颌第三磨牙远中根部,向后上走形,止于磨牙后区;③C型为高位型,该型自下颌管起始处附近即发出分支,向前走形,终止于磨牙后区或下颌支部位。Patil分类法简洁明了,能够清晰显示磨牙后管在下颌骨矢状面方向走形,但其分型局限于二维层面,无法判断磨牙后管在下颌骨颊舌侧位置。本研究在Patil分类法基础上于三维空间内对磨牙后管进行分型,将磨牙后管按照所在区域总体分为A、B两型,进而依据磨牙后管走形及颊舌侧位置作出进一步分型,相较传统分型更为明确细致,且三维分型能直观展示磨牙后管位置,指导临床相对传统分型更具有可靠性。

本研究中磨牙后管发生率为22.83%,与西班牙^[18]、伊朗^[7]及中国东部地区^[19]较为接近,高于我国台湾地区的10.3%^[20],这可能与我国台湾地区喜

好软食,食物加工较为精细,颌骨发育相对窄小有关,另外,与CBCT精确度、种族、环境差异相关。磨牙后管起始位置中心点距颊侧骨壁的水平距离平均为 (7.30 ± 1.99) mm,磨牙后管起始位置中心点距舌侧骨壁的水平距离平均为 (3.51 ± 1.04) mm,磨牙后管起始位置中心点距颊舌侧骨壁的水平距离差异有统计学意义;磨牙后孔中心点距颊侧骨壁的垂直距离平均为 (8.22 ± 2.18) mm,磨牙后孔中心点距舌侧骨壁的垂直距离平均为 (3.87 ± 1.77) mm,磨牙后孔中心点距颊舌侧骨壁的垂直距离差异有统计学意义。磨牙后管在A区和B区占比分别为65.42%、34.58%,差异有统计学意义。综上,本研究结果表明在山西人群中磨牙后管常起自下颌支部位,沿下颌骨内侧弯曲向上走形。这与Nikkerdar等^[7]、Patil等^[17]研究结果一致,但其研究发现一种特殊类型,该型直接连通第三磨牙远中牙周间隙与磨牙后区,此型在山西人群中暂未发现。磨牙后管各分型中A3型最为多见,其次是B3型,A4型最少见。在山西年龄 ≥ 18 周岁人群中,行下颌支截骨术、肿瘤切除术及下颌支部位骨折切开复位内固定术时应注意A型磨牙后管存在,行下颌支矢状劈开术前应根据磨牙后管颊舌侧位置设计切口及截骨位置,其中A3型磨牙后管最为常见,截骨位置应偏向下颌支颊侧面,避免损伤此型磨牙后管;行下颌支前缘取骨术及骨折手术时应注意A2、A5型磨牙后管存在;行复杂骨埋伏阻生智齿拔除术、磨牙区种植手术及复杂骨增量技术时应注意B型磨牙后管存在,根据牙体位置及磨牙后管走形设计切口、去骨范围,选择种植位点时应避开磨牙后管;行磨牙后区取骨术时靠近外斜线位置,应注意B4、B2型磨牙后管存在。

磨牙后管在性别、侧别间差异无统计学意义,这与其他研究^[7,20-22]结果一致。但有研究显示磨牙后管右侧多于左侧^[23],导致这种结果的原因目前尚不明确。各年龄组间磨牙后管发生率差异无统计学意义,这与其他学者研究结果一致^[24-25],但江西地区的研究显示下颌管分支发生率随年龄增长呈下降趋势,推测可能与基因、种族相关^[26]。

3.3 磨牙后管临床意义

磨牙后管位于磨牙后区或下颌升支部位,其内包含有来源于下颌管的有髓神经纤维及血管,磨牙后管损伤也会导致术区出血、感觉异常以及创伤性神经瘤等并发症的发生,因此明确磨牙后管的走形及管径大小十分重要,在磨牙后区行自

体骨移植取骨术或行下颌支矢状劈开术时应控制好手术部位及深度,防止损伤磨牙后管^[27]。磨牙后管内有髓神经纤维可支配磨牙后区及下颌磨牙、前磨牙及其颊侧牙龈感觉,因此磨牙后管的存在会影响下牙槽神经阻滞麻醉的成功率。有患者行下牙槽神经阻滞麻醉术后下唇及颊部麻木,而磨牙区颊侧黏膜及牙齿仍有痛觉,这种疼痛被称为“逃逸痛”。这类情况应考虑磨牙后管的存在,此时若加大阻滞麻醉注射剂量易导致患者出现麻药过量反应,正确做法是追加磨牙后管浸润麻醉,可显著提高麻醉成功率^[28]。在涉及阻生第三磨牙拔除时术前应通过CBCT确认磨牙后管位置,确定手术切口位置及翻瓣去骨范围,避免术中术后并发症发生。有学者在磨牙区种植位点发现下颌管分支结构,因此术前应拍摄CBCT排除磨牙后管存在,确定安全的手术区域。同时磨牙后管也可作为感染、肿瘤扩散的通道,颌骨恶性肿瘤涉及磨牙后区时应注意磨牙后管的存在,手术过程中应将磨牙后管一并去除^[19]。此外,牙槽骨高度会随年龄增长逐渐降低,老年人磨牙后管内容物易暴露在牙槽骨表面。在涉及磨牙后区的义齿修复时,应避开磨牙后管位置,防止压迫神经产生不适或者痛感。

【Author contributions】 Gong QN processed the research, analyzed the data and wrote the article. Wang J revised the article. Fan YW designed the study and revised the article. All authors read and approved the final manuscript as submitted.

参考文献

- [1] Zhou X, Gao X, Zhang J. Bifid mandibular canals: CBCT assessment and macroscopic observation[J]. *Surg Radiol Anat*, 2020, 42(9): 1073-1079. doi: 10.1007/s00276-020-02489-5.
- [2] Naitoh M, Hiraiwa Y, Aimiya H, et al. Observation of bifid mandibular canal using cone-beam computerized tomography[J]. *Int J Oral Maxillofac Implants*, 2009, 24(1): 155-159.
- [3] de Gringo CPO, de Gittins EVCD, Rubira CMF. Prevalence of retromolar canal and its association with mandibular molars: study in CBCT[J]. *Surg Radiol Anat*, 2021, 43(11): 1785 - 1791. doi: 10.1007/s00276-021-02787-6.
- [4] von Arx T, Bornstein MM. The bifid mandibular canal in three-dimensional radiography: morphologic and quantitative characteristics[J]. *Swiss Dent J*, 2021, 131(1): 10-28.
- [5] Okumuş Ö, Dumlu A. Prevalence of bifid mandibular canal according to gender, type and side[J]. *J Dent Sci*, 2019, 14(2): 126-133. doi: 10.1016/j.jds.2019.03.009.
- [6] Moreno Rabie C, Vranckx M, Rusque MI, et al. Anatomical relation of third molars and the retromolar canal[J]. *Br J Oral Maxillofac Surg*, 2019, 57(8): 765-770. doi: 10.1016/j.bjoms.2019.07.006.

- [7] Nikkerdar N, Golshah A, Norouzi M, et al. Incidence and anatomical properties of retromolar canal in an Iranian population: a cone-beam computed tomography study[J]. *Int J Dent*, 2020, 2020: 9178973. doi: 10.1155/2020/9178973.
- [8] Elnadoury EA, Gaweesh YSE, Abu El Sadat SM, et al. Prevalence of bifid and trifid mandibular canals with unusual patterns of nerve branching using cone beam computed tomography[J]. *Odontology*, 2022, 110(1): 203-211. doi: 10.1007/s10266-021-00638-9.
- [9] Chávez-Lomeli ME, Mansilla Lory J, Pompa JA, et al. The human mandibular canal arises from three separate canals innervating different tooth groups[J]. *J Dent Res*, 1996, 75(8): 1540-1544. doi: 10.1177/00220345960750080401.
- [10] Nithya J, Aswath N. Assessing the prevalence and morphological characteristics of bifid mandibular canal using cone-beam computed tomography - a retrospective cross-sectional study[J]. *J Clin Imaging Sci*, 2020, 10: 30. doi: 10.25259/JCIS_67_2019.
- [11] Komarnitki I, Mańkowska-Pliszka H, Roszkiewicz P, et al. A morphological study of retromolar foramen and retromolar canal of modern and medieval population[J]. *Folia Morphol (Warsz)*, 2019, 79(3):580-587. doi: 10.5603/FM.a2019.0124.
- [12] Kristen RR. The neurovascular contents of a unilateral double mandibular canal: a case study[J]. *FASEB J*, 2019, 33(S1): 616.12. doi: 10.1096/fasebj.2019.33.1_supplement.616.12
- [13] Do Q, Shen D, Ohyama H, et al. A rare case of trifid mandibular canal with bilateral retromolar foramina[J]. *Anat Cell Biol*, 2020, 53(4): 512-515. doi: 10.5115/acb.20.153.
- [14] Cha JY, Yoon HI, Yeo IS, et al. Panoptic segmentation on panoramic radiographs: deep learning-based segmentation of various structures including maxillary sinus and mandibular canal[J]. *J Clin Med*, 2021, 10(12): 2577. doi: 10.3390/jcm10122577.
- [15] Miličević A, Salarić I, Đanić P, et al. Anatomical variations of the bifid mandibular canal on panoramic radiographs in citizens from Zagreb, Croatia[J]. *Acta Stomatol Croat*, 2021, 55(3): 248 - 255. doi: 10.15644/asc55/3/2.
- [16] Ruetters M, Kim TS, Hagenfeld D, et al. *Ex vivo* assessment of the buccal and oral bone by CBCT[J]. *J Orofac Orthop*, 2021. doi: 10.1007/s00056-021-00335-w.
- [17] Patil S, Matsuda Y, Nakajima K, et al. Retromolar canals as observed on cone - beam computed tomography: their incidence, course, and characteristics[J]. *Oral Surg Oral Med Oral Pathol Oral Radiol*, 2013, 115(5): 692-699. doi: 10.1016/j.oooo.2013.02.012.
- [18] Puche -Roses M, Blasco -Serra A, Valverde -Navarro AA, et al. Prevalence and morphometric analysis of the retromolar canal in a Spanish population sample: a helical CT scan study[J]. *Med Oral Patol Oral Cir Bucal*, 2022, 27(2): e142-e149. doi: 10.4317/med-oral.25069.
- [19] Hou Y, Feng G, Lin W, et al. Observation of retromolar canals on cone beam computed tomography[J]. *Oral Radiol*, 2020, 36(4): 365-370. doi: 10.1007/s11282-019-00414-0.
- [20] Shen YW, Chang WC, Huang HL, et al. Assessment of the retromolar canal in Taiwan subpopulation: a cross-sectional cone-beam computed tomography study in a medical center[J]. *Tomography*, 2021, 7(2): 219-227. doi: 10.3390/tomography7020020.
- [21] Badry M, El-Badawy FM, Hamed WM. Incidence of retromolar canal in Egyptian population using CBCT: a retrospective study[J]. *Egypt J Radiol Nuc Med*, 2020, 51(1): 1-8. doi: 10.1186/s43055-020-00162-w.
- [22] Luangchana P, Pornprasertsuk -Damrongri S, Kitisubkanchana J, et al. The retromolar canal and its variations: classification using cone beam computed tomography[J]. *Quintessence Int*, 2018, 49(1): 61-67. doi: 10.3290/j.qi.a39224.
- [23] Han SS, Hwang YS. Cone beam CT findings of retromolar canals in a Korean population[J]. *Surg Radiol Anat*, 2014, 36(9): 871 - 876. doi: 10.1007/s00276-014-1262-1.
- [24] Rothe TM, Kumar P, Shah N, et al. Prevalence of bifid mandibular canal amongst Indian population: a radiographic study[J]. *J Maxillofac Oral Surg*, 2018, 17(3): 379-382. doi: 10.1007/s12663-017-1059-y.
- [25] Zhang YQ, Zhao YN, Liu DG, et al. Bifid variations of the mandibular canal: cone beam computed tomography evaluation of 1 000 Northern Chinese patients[J]. *Oral Surg Oral Med Oral Pathol Oral Radiol*, 2018, 126(5): e271 - e278. doi: 10.1016/j.oooo.2018.06.008.
- [26] 柯星, 李博涵, 陈林林, 等. 江西成年人群下颌骨体副孔解剖位置的锥形束CT研究[J]. *华西口腔医学杂志*, 2017, 35(6): 607-612. doi: 10.7518/hxkq.2017.06.009.
- Ke X, Li BH, Chen LL, et al. A cone beam computed tomography study on the anatomical position of accessory mandibular foramina in Jiangxi adults[J]. *West Chin J Stomatol*, 2017, 35(6): 607-612. doi: 10.7518/hxkq.2017.06.009.
- [27] 戴昱, 张国志, 孙海鹏. 锥形束CT观测下牙槽神经管分支[J]. *口腔疾病防治*, 2018, 26(2): 113-116. doi: 10.12016/j.issn.2096-1456.2018.02.009.
- Dai Y, Zhang GZ, Sun HP. The observation of bifid mandibular canals using cone beam computed tomography[J]. *J Prev Treat Stomatol Dis*, 2018, 26(2): 113 - 116. doi: 10.12016/j.issn.2096-1456.2018.02.009.
- [28] Costa ED, Peyneau PD, Visconti MA, et al. Double mandibular canal and triple mental foramina: detection of multiple anatomical variations in a single patient[J]. *Gen Dent*, 2019, 67(5): 46-49.

(编辑 周春华)



官网